

This material is posted here with permission of the IEEE. Such permission of the IEEE does not in any way imply IEEE endorsement of any of Helsinki University of Technology's products or services. Internal or personal use of this material is permitted. However, permission to reprint/republish this material for advertising or promotional purposes or for creating new collective works for resale or redistribution must be obtained from the IEEE by writing to [pubs-permissions@ieee.org](mailto:pubs-permissions@ieee.org).

By choosing to view this document, you agree to all provisions of the copyright laws protecting it.

## Effect of Ni on the formation of $\text{Cu}_6\text{Sn}_5$ and $\text{Cu}_3\text{Sn}$ intermetallics

Hao Yu, Vesa Vuorinen and Jorma Kivilahti  
Lab. of Electronics Production Technology  
Helsinki University of Technology  
P.O.Box 3000, FIN-02015 HUT, Finland  
Contact E-mail: jorma.kivilahti@hut.fi

### Abstract

In this paper, the effect of Ni on the formation of  $\text{Cu}_6\text{Sn}_5$  and  $\text{Cu}_3\text{Sn}$  intermetallics between tin and (Cu,Ni)-substrates has been studied by making use of the thermodynamic assessment of the Sn-Cu-Ni system. The driving forces for the diffusion of the elements in the intermetallic layers were calculated as a function of Ni-content. Assuming constant mobilities of component atoms, the results suggest that the diffusion fluxes of all the components in the  $(\text{Cu,Ni})_6\text{Sn}_5$  layer increase with increasing content of dissolved Ni, while the Cu and Sn fluxes in the  $(\text{Cu,Ni})_3\text{Sn}$  layer decrease. Therefore, the dissolution of Ni retards the growth of  $(\text{Cu,Ni})_3\text{Sn}$ . When the Ni-content of the (Cu,Ni) substrate is high enough, the intermetallic compound growth in the reaction zones is dominated by  $(\text{Cu,Ni})_6\text{Sn}_5$  and the  $(\text{Cu,Ni})_3\text{Sn}$  layer disappears gradually. The small thickness of  $(\text{Cu,Ni})_3\text{Sn}$  is associated with large difference between Sn and Cu fluxes in  $(\text{Cu,Ni})_3\text{Sn}$  that encourages also the “Kirkendall void” formation. In addition, the calculated driving forces suggest that the growth rate of  $(\text{Cu,Ni})_6\text{Sn}_5$  should further increase if  $(\text{Cu,Ni})_3\text{Sn}$  disappears, resulting in an unusually thick  $(\text{Cu,Ni})_6\text{Sn}_5$  layer. The results of thermodynamic calculations supplemented with diffusion kinetic considerations are in good agreements with recent experimental observations.

### Introduction

Nickel can be present in solder interconnections due to its dissolution from printed wiring boards' (PWB) metal finish or from under bump metallizations (UBM) of components. More recently, Ni is also used as a minor alloying element in solder pastes in order to improve the reliability against mechanical shocks<sup>1,2</sup>. It has been argued that Ni alloying alters significantly the microstructures of near-eutectic SnAgCu interconnections. For example, the addition of Ni has been claimed to refine the IMC precipitates in the Sn-Ag-Cu solder<sup>3</sup> and to enhance the growth of interfacial intermetallic compound (IMC)<sup>4</sup>. On the other hand, Ni is known to have negative effect on the reliability, when it is dissolved extensively into  $(\text{Cu,Ni})_6\text{Sn}_5$ <sup>5</sup>. To obtain a better understanding of why and how Ni is affecting the reliability of solder interconnections, the mechanisms behind these microstructural changes need to be clarified.

In order to study the influences of any alloying element, M, reliable thermodynamic description of the ternary Sn-Cu-M system is required. Without knowing the thermodynamic properties of the corresponding phases, it is not possible to carry out detailed kinetic analyses for improving the understanding of the formation of IMC structures<sup>6</sup>. Hence, the assessment of the thermodynamic properties of the Sn-Cu-Ni system becomes necessary.

It is known that  $\text{Cu}_6\text{Sn}_5$  tends to dissolve large amounts of Ni<sup>7</sup>. In a recent study with the solid-state Sn|(Cu,Ni) diffusion couples, it was found that the growth of  $(\text{Cu,Ni})_6\text{Sn}_5$  was significantly accelerated by small amounts of Ni alloyed in copper substrate and this increase was accompanied with an increasing number of voids in the  $\text{Cu}_3\text{Sn}$  layer<sup>8</sup>. However, further increase of Ni-content in the substrate suppressed the formation of  $\text{Cu}_3\text{Sn}$  layer and, naturally, eliminated the voids. Our experiments carried out at the lower temperature ( $T = 125^\circ\text{C}$ ) showed the similar effect of Ni (see Figs. 1(a) and 1(b))<sup>9</sup>. A reasonable explanation would be that the growth of  $(\text{Cu,Ni})_6\text{Sn}_5$  is so

fast that it becomes dominant in the IMC layers. Recently, we have also observed very fast growth of  $(\text{Cu,Ni})_6\text{Sn}_5$  and the absence of  $(\text{Cu,Ni})_3\text{Sn}$  in the liquid-solid Sn|(Cu,Ni) reaction couples<sup>10</sup>. For example, Fig. 2 shows the interfacial reaction zone of Sn|95Cu5Ni (at-%) reaction couples after reflow soldering [ $T_{\text{peak}}=260^\circ\text{C}$ ,  $t_{\text{liquid}} (T>232^\circ\text{C}) \sim 40\text{s}$ ].

In this paper we aim to study theoretically the experimental observations on the effects of Ni on the formation of  $\text{Cu}_6\text{Sn}_5$  and  $\text{Cu}_3\text{Sn}$  by making use of the thermodynamic properties of the Sn-Cu-Ni system and diffusion kinetic considerations.

## Thermodynamic Properties of the Sn-Cu-Ni System

For the Sn-Cu-Ni system, all the three binary systems Sn-Cu<sup>11</sup>, Sn-Ni<sup>12,13</sup> and Cu-Ni have been assessed previously and their descriptions are available in the literature. In this work, they are adopted with some necessary modifications in order to make the models in different binary systems consistent.

The Sn-Cu-Ni system has not been completely assessed earlier. A partial assessment of Sn-Cu-Ni system has been carried out by Miettinen<sup>14</sup> and it is valid only in the Cu-Ni side up to  $x_{\text{Sn}}=0.25$ . The experimental data available in the Cu-Ni side of the system<sup>15</sup>, including the information from the  $\text{Cu}_3\text{Sn-Ni}_3\text{Sn}$  isopleth<sup>16</sup> are considered in his assessment. However, the phases commonly found in solder interconnections,  $\text{Cu}_6\text{Sn}_5$  and  $\text{Ni}_3\text{Sn}_4$ , were not included. The extension of such description to Sn-rich region is therefore needed.

Such an extension is recently enabled by some experimental investigations in the Sn-rich region, including the isothermal sections at  $800^\circ\text{C}$ ,  $240^\circ\text{C}$ ,  $235^\circ\text{C}$  proposed by Wang and Chen<sup>17</sup>, Lin et al<sup>18</sup> and Oberndorff<sup>19</sup>. Oberndorff reported a ternary phase  $45\text{Sn}29\text{Cu}26\text{Ni}$ , which might be stable but unlikely to exist in solder interconnections. From the practical point of view, it is out of our interest and the results from the other two studies were used in this work.

Some studies on the interfacial reactions also offered phase equilibrium information in the Sn-Cu-Ni system. Chen et al<sup>20</sup> examined the intermetallic formation at the interfaces in a multilayer Sn/Cu/Sn/Ni/Sn/Cu/Sn specimen at  $240^\circ\text{C}$ ; Ho et al<sup>21</sup> investigated the formations of  $\text{Cu}_6\text{Sn}_5$  and  $\text{Ni}_3\text{Sn}_4$  at liquid solder/Ni substrate interface. The data from these researches were also used in our assessment.

With the description of the ternary Sn-Cu-Ni system obtained, both the thermodynamic properties of the phases and the ternary phase diagram can be calculated and compared with experimental data. In the Cu-Ni side, all the results previously presented by Miettinen<sup>14</sup> can be reproduced. The agreement between experimental data and calculated results in the Sn-rich region is also satisfactory. Fig.3 presents the calculated isothermal section at  $240^\circ\text{C}$ , which is one of the most important isothermal sections in studying the interfacial reactions during reflow soldering. More details of the assessment and the thermodynamic parameters obtained are presented elsewhere<sup>22</sup>.

## Driving Forces for Diffusion

Growth rates of IMC layers in interfacial reactions are determined by the diffusion fluxes through different reaction layers. The layers with high diffusion rates of elements tend to grow fast and sometimes suppress the growth of the other layers. The diffusion flux of an element  $i$  through a thin layer of thickness  $\delta$  is often presented by its diffusion coefficient  $D_i$  and concentration gradient  $\Delta C_i/\delta$  according to the Fick's first law,

$$J_i = D_i \frac{\Delta C_i}{\delta} \quad (1)$$

However, in the case of intermetallic layers of limited homogeneity range, it is more convenient to replace the concentration gradient by chemical potential gradient. Atom mobility should be used instead of diffusion coefficient accordingly. The diffusion flux is then presented as:

$$J_i = C_i M_i \frac{\Delta G_i}{\delta} = \frac{M_i x_i \Delta G_i}{\delta V} \quad (2)$$

Where  $C_i$  and  $x_i$  are the concentration and atomic fraction of element  $i$ ,  $M_i$  is the mobility of  $i$ ,  $V$  is the molar volume of the layer.  $\Delta G_i$  denotes the chemical potential difference and its gradient,  $\Delta G_i/\delta$ , is the driving force for diffusion.

With the thermodynamic description of the Sn-Cu-Ni system obtained above, the chemical potential differences can be easily computed, if local (stable or metastable) equilibrium is assumed at interfaces. Fig.4 shows the calculated Gibbs energy curves of the phases in Sn|Cu diffusion couple at 240°C. At the Liquid(Sn)/Cu<sub>6</sub>Sn<sub>5</sub> interface, the compositions of both phases are determined by the common tangent line AB to their Gibbs energy curves. The y coordinates of points A and B are the chemical potentials of Sn and Cu at the interface. Similarly, points C and D determine the chemical potentials at the Cu<sub>6</sub>Sn<sub>5</sub>/Cu<sub>3</sub>Sn interface. Hence, the length of AC is the difference of Sn potential and the length of BD is the difference of Cu potential over Cu<sub>6</sub>Sn<sub>5</sub>,

$$\begin{aligned} \Delta G_{Sn}^{Cu_6Sn_5} &= G_{Sn}^{Sn/Cu_6Sn_5} - G_{Sn}^{Cu_6Sn_5/Cu_3Sn} \\ \Delta G_{Cu}^{Cu_6Sn_5} &= G_{Cu}^{Cu_6Sn_5/Cu_3Sn} - G_{Cu}^{Sn/Cu_6Sn_5} \end{aligned} \quad (3)$$

When Ni is present, it dissolves into both compounds and the Gibbs energy curves in Fig.4 turn into surfaces in the ternary system. Phase equilibrium is decided by common tangent planes instead and Ni flux is also originated by its potential difference:

$$\Delta G_{Ni}^{Cu_6Sn_5} = G_{Ni}^{Cu_6Sn_5/Cu_3Sn} - G_{Ni}^{Sn/Cu_6Sn_5} \quad (4)$$

In ternary phase diagram, the compositions of two equilibrated phases form a tieline in the corresponding isothermal section. Such tielines are not unique so that different interfacial compositions are possible, resulting in different chemical potentials of elements at the interface. For example, at the (Cu,Ni)<sub>6</sub>Sn<sub>5</sub>/(Cu,Ni)<sub>3</sub>Sn interface, interfacial compositions may follow any of the tielines between (Cu,Ni)<sub>6</sub>Sn<sub>5</sub> and (Cu,Ni)<sub>3</sub>Sn, depending on Ni-content. It is the same for the other interfaces in the reaction zone, so the chemical potential differences over intermetallic layers are functions of Ni-content. The calculated results at 240°C are shown in Fig.5. Similar results have been also obtained for solid-state diffusion couples at 125°C.

The chemical potential differences in Fig.5 are plotted against the mole fraction of Ni in the compounds. Since the compositions of (Cu,Ni)<sub>6</sub>Sn<sub>5</sub> and (Cu,Ni)<sub>3</sub>Sn are determined by the tielines between them in Fig.3, there is an direct correlation between the mole fractions of Ni in (Cu,Ni)<sub>6</sub>Sn<sub>5</sub> and (Cu,Ni)<sub>3</sub>Sn. Once the mole fraction of Ni in (Cu,Ni)<sub>3</sub>Sn is known, the mole fraction of Ni in (Cu,Ni)<sub>6</sub>Sn<sub>5</sub> is fixed and vice versa.. By this means, the impacts of Ni on the diffusion fluxes in both intermetallic layers, for example, the results in Fig.5(a) and Fig.5(b), can be correlated with each other. Since the Ni solubility in (Cu,Ni)<sub>3</sub>Sn is remarkably smaller than the corresponding Ni solubility in (Cu,Ni)<sub>6</sub>Sn<sub>5</sub>, the plotted range of Ni solubility in Fig.5(a) and Fig.5(b) is relatively narrow and only up to 0.09.

As shown in Fig.5, the driving forces of the diffusion in (Cu,Ni)<sub>6</sub>Sn<sub>5</sub> increase with Ni-content, while those in (Cu,Ni)<sub>3</sub>Sn decrease due to the addition of Ni.

The values of driving forces are related to the changes in the interfacial layers. When Ni-content is high, it has been observed that (Cu,Ni)<sub>3</sub>Sn disappears from the reaction zone. Under such

situations,  $(\text{Cu,Ni})_6\text{Sn}_5$  becomes in direct contact with the substrate and the interfacial chemical potentials are determined by the metastable fcc/ $(\text{Cu,Ni})_6\text{Sn}_5$  equilibrium. The potential differences over  $(\text{Cu,Ni})_6\text{Sn}_5$  layer are changed accordingly. Simply as an example, if  $\text{Cu}_3\text{Sn}$  would not form in binary  $\text{Cu}|\text{Sn}$  diffusion couple for some reason, Sn and Cu potential differences over  $\text{Cu}_6\text{Sn}_5$  were represented by the lengths of AC' and BD' in Fig.4 instead. The corresponding results in the ternary system are shown (thin lines with symbols) in Fig.5a.

### Influence of Ni on Interfacial Reactions

Diffusion flux, as shown in Equation (2), is a function of chemical potential gradient, molar volume of compound, mobility and atomic fraction. However, if we assume the elements' mobilities and molar volumes are not significantly dependent of Ni-content, when the layer is having a specific thickness, the diffusion fluxes are approximately proportional to the product of the mole fraction of diffusing element and its chemical potential difference:

$$J_i \propto x_i \Delta G_i \quad (5)$$

In the experimental investigation on Kirkendall planes, Paul reported that the ratios of intrinsic diffusivities of Cu and Sn in  $(\text{Cu,Ni})_3\text{Sn}$  layer are similar in  $\text{Sn}|\text{Cu}$  and  $\text{Sn}|\text{99Cu1Ni}$  diffusion couples<sup>8</sup>, which indicates that the mobilities of elements do not vary abruptly with Ni-content. Hence, as a first approximation, the function  $x_i \Delta G_i$  can be used as a variable causing the relative change of diffusion flux upon Ni dissolution.

The calculated  $x_i \Delta G_i$ -functions for the diffusion fluxes in liquid-solid  $\text{Sn}|\text{(Cu,Ni)}$  reaction couple at 240°C are shown in Fig.6. The results for solid-state  $\text{Sn}|\text{(Cu,Ni)}$  diffusion couple are quite similar. The  $x_i \Delta G_i$ -functions for all the diffusion fluxes in  $(\text{Cu,Ni})_6\text{Sn}_5$  significantly increase with the addition of Ni. In the  $(\text{Cu,Ni})_3\text{Sn}$  layer, the  $x_i \Delta G_i$ -functions for the Sn and Cu fluxes decrease and that for Ni flux slightly increase with Ni-content.

#### 1) Shrinkage of $(\text{Cu,Ni})_3\text{Sn}$ layer

The changes of the diffusion fluxes as functions of Ni dissolution would lead to the domination of  $(\text{Cu,Ni})_6\text{Sn}_5$ . In the study on binary  $\text{Sn}|\text{Cu}$  diffusion couples, Paul et al analyzed the growth kinetics of  $\text{Cu}_6\text{Sn}_5$  and  $\text{Cu}_3\text{Sn}$  layers by measuring the position of Kirkendall planes with inert markers<sup>23</sup>. Based on this work, the following equation can be derived to evaluate the thickness of  $\text{Cu}_3\text{Sn}$  layer:

$$\delta_{\text{Cu}_3\text{Sn}} = \frac{8}{9} t V_{\text{Cu}_3\text{Sn}} \varphi \quad (6)$$

$$\varphi = 5J_{\text{Cu}}^{\text{Cu}_3\text{Sn}} + 15J_{\text{Sn}}^{\text{Cu}_3\text{Sn}} - 5J_{\text{Cu}}^{\text{Cu}_6\text{Sn}_5} - 6J_{\text{Sn}}^{\text{Cu}_6\text{Sn}_5}$$

where  $t$  is time,  $V_{\text{Cu}_3\text{Sn}}$  is the molar volume of  $\text{Cu}_3\text{Sn}$ ,  $J_i^M$  is the flux of element  $i$  through the IMC layer M.  $\varphi$  determines the growth rate of  $\text{Cu}_3\text{Sn}$  layer and it is positive in binary  $\text{Sn}|\text{Cu}$  diffusion couple.

In  $\text{Sn}|\text{(Cu,Ni)}$  diffusion couple, Ni fluxes in both layers have impacts on  $\varphi$ . Since Ni substitute Cu in both compounds, the expression for the function  $\varphi$  is as follow:

$$\varphi = 5\left(J_{\text{Cu}}^{\text{Cu}_3\text{Sn}} + J_{\text{Ni}}^{\text{Cu}_3\text{Sn}}\right) + 15J_{\text{Sn}}^{\text{Cu}_3\text{Sn}} - 5\left(J_{\text{Cu}}^{\text{Cu}_6\text{Sn}_5} + J_{\text{Ni}}^{\text{Cu}_6\text{Sn}_5}\right) - 6J_{\text{Sn}}^{\text{Cu}_6\text{Sn}_5} \quad (7)$$

According to our calculated  $x_i\Delta G_i$ -functions, all the diffusion fluxes except  $J_{Ni}^{Cu_3Sn}$  vary in a manner that  $\phi$  value decreases with increasing Ni-content. Because the Ni-content in  $(Cu,Ni)_3Sn$  is low,  $J_{Ni}^{Cu_3Sn}$  plays a less important role in the equation and thus  $\phi$  value is expected to decrease, which means that the growth of  $Cu_3Sn$  layer slows down. When Ni-content reaches a critical level, the effect of Ni would be so significant that  $\phi$  becomes negative and  $Cu_3Sn$  does not form in the reaction zone. This explained why the formation of  $(Cu,Ni)_3Sn$  was suppressed in both liquid-solid and solid-state reaction couples. Although no quantitative evaluation on such critical Ni-content in substrate is possible due to the lack of kinetic data, it is possibly around 5 at.% according to experimental observations, as shown in Fig.2.

## 2) Kirkendall voids in $(Cu,Ni)_3Sn$ layer

The Kirkendall voids occurring in  $(Cu,Ni)_3Sn$  layer is the result of unequal intrinsic flux of Cu and Sn in  $Cu_3Sn$  layer. It is known that long time annealing causes voiding in binary Sn|Cu diffusion couples. Paul et al extracted the value  $J_{Sn}^{Cu_3Sn} / J_{Cu}^{Cu_3Sn} = 0.9$  from the experimental Cu| $Cu_6Sn_5$  diffusion couple results<sup>8</sup>. According to our results in Fig.6(b), when a small amount of Ni dissolves into  $(Cu,Ni)_3Sn$ , the  $x_i\Delta G_i$ -function for Cu flux decreases slightly faster than that for Sn flux, but this accompanied with an increase of the  $x_i\Delta G_i$ -function for Ni flux. As a result, there are two opposite influences on the ratio  $J_{Sn}^{Cu_3Sn} / (J_{Cu}^{Cu_3Sn} + J_{Ni}^{Cu_3Sn})$  from the variations of Cu flux and Ni flux. Although they do not compensate exactly with each other, it can be expected that  $J_{Sn}^{Cu_3Sn} / (J_{Cu}^{Cu_3Sn} + J_{Ni}^{Cu_3Sn})$  do not change significantly with the existence of Ni. Hence, the variation of  $J_{Sn}^{Cu_3Sn} / (J_{Cu}^{Cu_3Sn} + J_{Ni}^{Cu_3Sn})$  ratio is not likely to play a major role in the acceleration of Kirkendall void formation.

Ni slows down the growth of  $(Cu,Ni)_3Sn$  and the resulted  $\delta_{Cu_3Sn}$  could be very small in Sn|(Cu,Ni) diffusion couple. Even though the ratio  $J_{Sn}^{Cu_3Sn} / (J_{Cu}^{Cu_3Sn} + J_{Ni}^{Cu_3Sn})$  remains at the same level in  $(Cu,Ni)_3Sn$ , since all the diffusion fluxes are inversely proportional to the layer thickness, the vacancy flux  $J_V = J_{Cu}^{Cu_3Sn} + J_{Ni}^{Cu_3Sn} - J_{Sn}^{Cu_3Sn}$  is inversely proportional to  $\delta_{Cu_3Sn}$ . Hence, the small thickness of  $(Cu,Ni)_3Sn$  layer according to our calculated  $x_i\Delta G_i$ -functions can explain the increase of the number of Kirkendall voids.

Due to the lack of data, the mobilities of the elements were assumed to be independent of Ni-content up to now. Since  $Ni_3Sn$  has much higher Gibbs (free) energy of formation than  $Cu_3Sn$ , Ni atoms have greater chemical affinity to Sn atoms than to Cu atoms. Therefore, we expect Ni atoms to reduce the mobility of Sn and to increase the mobility of Cu in the  $(Cu,Ni)_3Sn$ . The difference between Cu and Sn fluxes in the  $(Cu,Ni)_3Sn$  layer can be even larger than we expect and the unusual number of ‘‘Kirkendall voids’’ can be even better explained with such an effect taken into account.

## 3) Enhanced growth of $(Cu,Ni)_6Sn_5$

When Ni-content is small, it can be seen in Fig.6(a) that the calculated  $x_i\Delta G_i$ -functions in  $(Cu,Ni)_6Sn_5$  layer could be 3-4 times larger simply due to the absence of  $(Cu,Ni)_3Sn$  layer. It means that the growth of  $(Cu,Ni)_6Sn_5$  can be further accelerated once  $(Cu,Ni)_3Sn$  has disappeared. In our recent study with liquid-solid Sn|(Cu,Ni) reaction couples at 240°C, interesting changes of the thickness of IMC layers have been observed. The extremely promoted  $(Cu,Ni)_6Sn_5$  thickness and the elimination of Kirkendall voids would have inverse impacts on interfacial reliability and it is thus of great importance to evaluate them in the future. For this purpose, the mechanism of the enhanced

growth of  $(\text{Cu,Ni})_6\text{Sn}_5$  proposed in the present calculation is helpful in understanding the phenomenon and more details will be presented elsewhere<sup>10</sup>.

## Conclusions

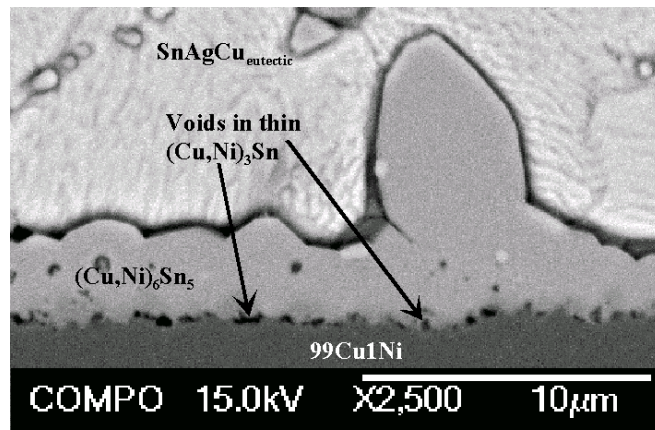
The influence of Ni on the formation of  $\text{Cu}_6\text{Sn}_5$  and  $\text{Cu}_3\text{Sn}$  layers between Sn-based solder and  $(\text{Cu,Ni})$  was studied by assessing first the thermodynamic properties of the Sn-Cu-Ni system and then calculating the driving forces for diffusion fluxes. If constant mobilities of component atoms are assumed in both  $(\text{Cu,Ni})_6\text{Sn}_5$  and  $(\text{Cu,Ni})_3\text{Sn}$ , the results suggest that the dissolution of Ni in the intermetallics increases all the diffusion fluxes in the  $(\text{Cu,Ni})_6\text{Sn}_5$  layer, while it decreases the diffusion rates of Sn and Cu and slightly adds up to that of Ni in the  $(\text{Cu,Ni})_3\text{Sn}$  layer. As a result, the  $(\text{Cu,Ni})_6\text{Sn}_5$  will become the dominant phase in the reaction zones, whereas the  $(\text{Cu,Ni})_3\text{Sn}$  gradually disappears from the interconnection structure, when Ni-content is high enough. Concurrently, the “Kirkendall void” formation will be faster in the progressively thinner  $(\text{Cu,Ni})_3\text{Sn}$  layer. It is also interesting to find out that the disappearance of  $(\text{Cu,Ni})_3\text{Sn}$  from the interconnection structure will further increase the driving forces for the diffusion of all the elements through  $(\text{Cu,Ni})_6\text{Sn}_5$  and thereby the growth rate of  $(\text{Cu,Ni})_6\text{Sn}_5$ . The above results are in agreement with recent experimental observations made from the Sn| $(\text{Cu,Ni})$  reaction couples.

## References

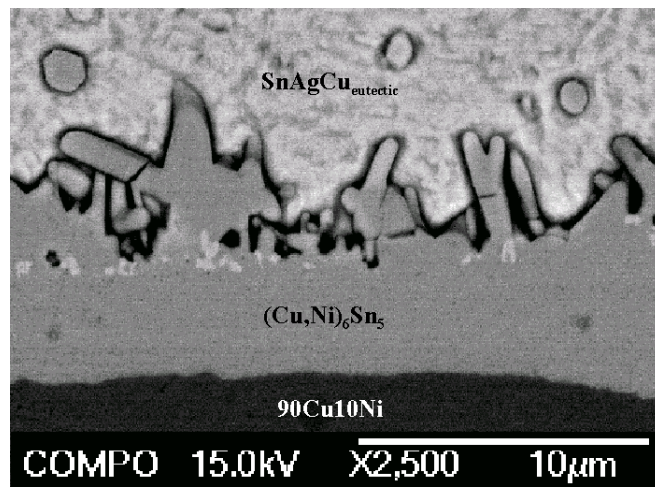
1. Terashima S., and Tanaka M., “Thermal Fatigue Properties of Sn-1.2Ag-0.5Cu-xNi Flip Chip Interconnects”, *Materials Transactions*, V45 (2004), No.3, 681-688.
2. Terashima S., Takahama K., Nozaki M., and Tanaka M., “Recrystallization of Sn Grains due to Thermal Strain in Sn-1.2Ag-0.5Cu-0.05Ni Solder”, *Materials Transactions*, V45 (2004), No.4, 1383-1390.
3. Kim K.S., Huh S.H., Sukanuma K., “Effects of fourth alloying additive on microstructures and tensile properties of Sn-Ag-Cu alloy and joints with Cu”, *Microelectronics Reliability* 43 (2003). 259-267
4. Chuang C-H., Lin K-L. “Effect of Microelements Addition on the Interfacial Reaction between Sn-Ag-Cu Solders and the Cu Substrate”, *Journal of Electronic Materials*. Vol. 32 (2003), No. 12, 1426-1431.
5. Mattila T.T. and Kivilahti J.K., “Reliability of Lead-free Interconnections under Consecutive Thermal and Mechanical Loadings”, *Journal of Electronics Materials*, Vol. 35 (2006), No.2, 250-256.
6. Kivilahti J., “The Chemical Modeling of Electronic Materials and Interconnections”, *Journal of Metals*, December 2002, 52-57.
7. Laurila T., Vuorinen V., and Kivilahti J.K., “Interfacial Reactions between Lead-free Solders and Common Base Materials”, *Materials Science & Engineering*, R 49, (2005), 1-60.
8. Paul A., “The Kirkendall Effect in Solid State Diffusion”, Doctoral Thesis, Eindhoven University of Technology, The Netherlands, 2004.
9. Hurtig J., M.Sc. Thesis, Helsinki University of Technology (2006).
10. V.Vuorinen, H.Yu and J.K.Kivilahti “Formation of the Intermetallic Compounds between Liquid Sn and Different  $\text{CuNix}$  Metallizations” (to be published).
11. Shim J.-H., Oh C.-S., Lee B.-J. and Lee D. N, “Thermodynamic Assessment of the Cu-Sn System”, *Z. Metallkd.*, Vol. 87 (1996), No.3, 205-212.
12. Ghosh G., “Thermodynamic Modeling of the Nickel-Lead-Tin System”, *Metallurgical and Materials Transaction* 30A (1999), No.1, 1481-1494.
13. Liu H.S., Wang J., and Jin Z.P., “Thermodynamic Optimization of the Ni-Sn Binary system”, *CALPHAD*, Vol.28, (2004), 363-370.

14. Miettinen J., "Thermodynamic Description of the Cu-Ni-Sn system at the Cu-Ni side", CALPHAD, Vol.27 (2003), 309-318.
15. Gupta K.P., "An expanded Cu-Ni-Sn System (Copper-Nickel-Tin)", Journal of Phase Equilibria, V21, (2000), No.5, 479-484.
16. Lee Pak J.S., Mukherjee K., "Phase Transformations in (Ni,Cu)<sub>3</sub>Sn Alloys", Materials Science and Engineering, A117 (1989), 167-173.
17. Wang C.-H. and Chen S.-W., "Isothermal Section of the Ternary Sn-Cu-Ni System and Interfacial Reactions in the Sn-Cu/Ni Couples at 800 °C", Metallurgical and Materials Transactions, 34A (2003), 2281-2287.
18. Lin C.-H., Chen S.-W., and Wang C.-H., "Phase Equilibrium and Solidification Properties of Sn-Cu-Ni alloys", Journal of Electronic Materials, Vol.31(2002), No.9, 907-915.
19. Oberndorff P., "Lead-free Solder Systems: Phase Relations and Microstructures", Doctoral Thesis, Eindhoven University of Technology, The Netherlands 2001.
20. Chen S.-W., Wu S.-H. and Lee S.-W., "Interfacial Reactions in the Sn-(Cu)/Ni, Sn-(Ni)/Cu and Sn/(Cu,Ni) Systems", J. Electronic Materials, Vol. 32 (2003), No.11, 1188-1194.
21. C.E. Ho, R. Y. Tsai, Y. L. Lin and C. R. Kao, "Effect of Cu Concentration on the Reaction on between Sn-Ag-Cu Solders and Ni", Journal of Electronic Materials, vol. 31, no. 6, 2002, pp 584-590.
22. H.Yu, V.Vuorinen and J.K.Kivilahti, "Solder/substrate interfacial reactions in Sn-Cu-Ni interconnection system", Journal of Electronic Materials (in print).
23. Paul A., Kodentsov A., van Loo F.J.J., "Intermetallic growth and Kirkendall effect manifestations in Cu/Sn and Au/Sn diffusion couples", Z. Metallkd., Vol.95, No.10, 913-920, (2004).





(a)



(b)

Fig.1 Reaction layers of (a) SnAgCu<sub>eut</sub>|99Cu1Ni (at-%) and (b) SnAgCu<sub>eut</sub>|90Cu10Ni (at-%) diffusion couples annealed at 125°C for 1000 hours.

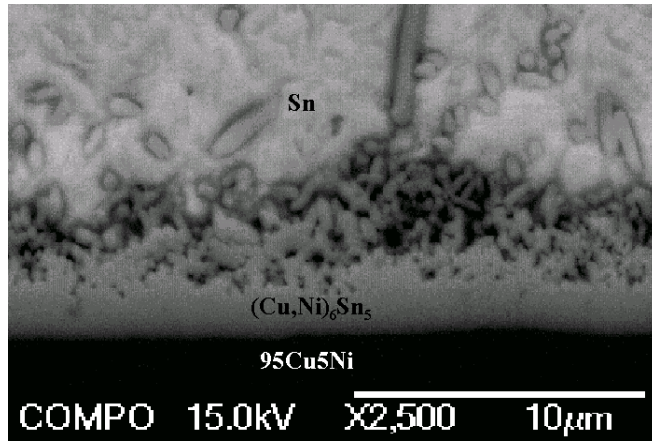


Fig.2 Reaction layers of Sn|95Cu5Ni (at-%) after reflow [ $T_{\text{peak}}=260^{\circ}\text{C}$ ,  $t_{\text{liquid}} (T > 232^{\circ}\text{C}) \sim 40\text{s}$ ]

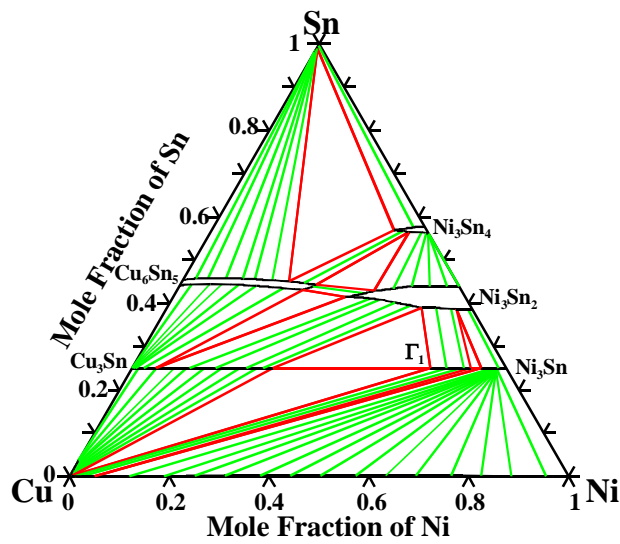


Fig.3 Calculated isothermal section of the Sn-Cu-Ni phase diagram at  $240^{\circ}\text{C}$ .

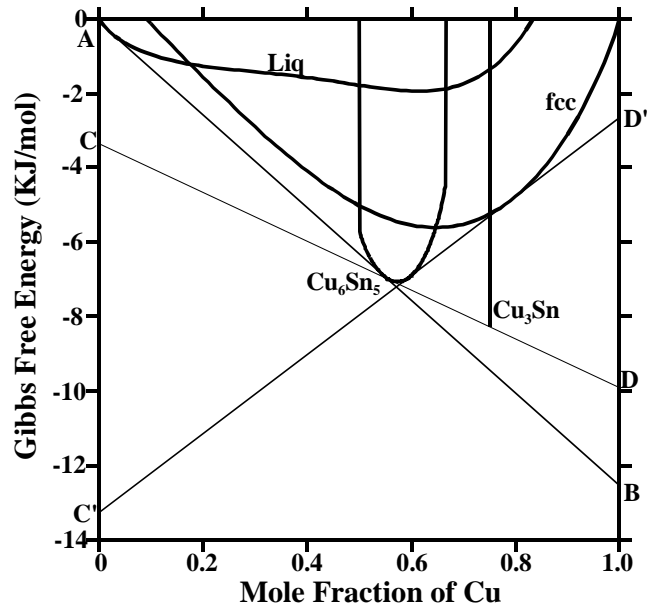
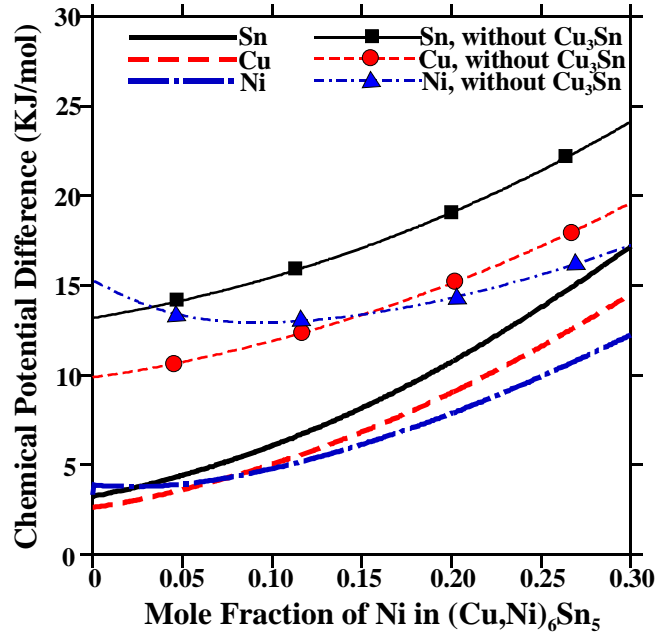
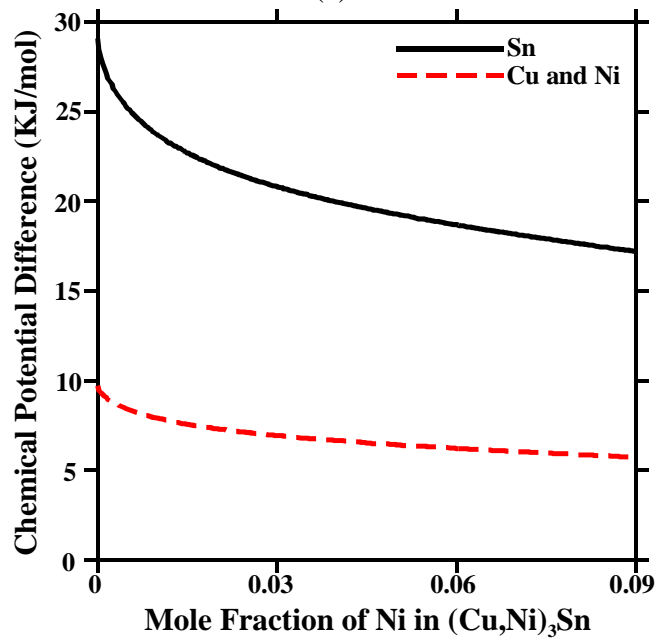


Fig.4 Calculated Gibbs free energies of liquid, fcc, Cu<sub>6</sub>Sn<sub>5</sub> and Cu<sub>3</sub>Sn at 240°C, showing how the chemical potential differences for diffusions are calculated in binary Sn-Cu system.



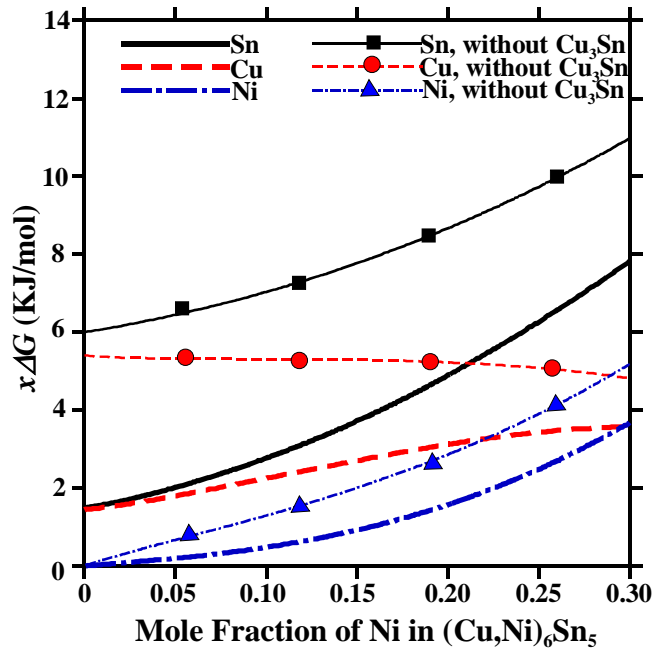
(a)



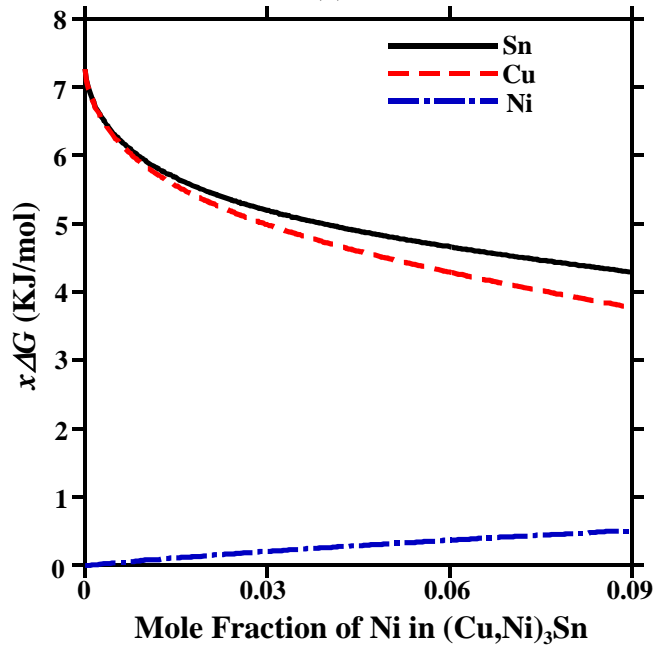
(b)

Fig.5 Calculated chemical potential differences over IMC layers in Sn|(Cu,Ni) diffusion couple at 240°C, whose gradients are the driving forces of diffusions.

(a)  $(\text{Cu,Ni})_6\text{Sn}_5$  (b)  $(\text{Cu,Ni})_3\text{Sn}$



(a)



(b)

Fig.6 Calculated  $x_i \Delta G_i$  for the diffusion fluxes in liquid-solid Sn|(Cu,Ni) diffusion couple at 240°C.  
 (a)  $(\text{Cu,Ni})_6\text{Sn}_5$  (b)  $(\text{Cu,Ni})_3\text{Sn}$